KERNFORSCHUNGSZENTRUM

KARLSRUHE

November 1972

Temperature and Heat-Flux Distribution in the Molten Core Mass
of a GCFR after a Hypothetical Melt-Down Accident

L. Barleon, M. Dalle Donne, S. Dorner

GESELLSCHAFT FÜR KERNFORSCHUNG M. B. H.
KARLSRUHE

KERNFORSCHUNGSZENTRUM KARLSRUHE

Institut für Neutronenphysik und Reaktortechnik

Projekt Schneller Brüter

Temperature and Heat-Flux Distribution in the Molten Core Mass of a
GCFR after a Hypothetical Melt-Down Accident.[*]

L.Barleon, M.Dalle Donne[**] and S.Dörner

Gesellschaft für Kernforschung mbH., Karlsruhe

Abstract

Although a simultaneous loss of both coolant pressure and all of the coolant circulations appears to be too unlikely in a properly designed GCFR-System as to be taken as design basis accident, the question about temperature and heat-flux distribution in the molten core mass containing in a Core-Catcher would be of great interest.

It was assumed in this paper that the molten core mass has reached the core catcher after 100 sec, and that the melt is separated into an oxide and a metallic phase.

Depending on their state, the fission products will be in the metallic or oxide melt and in the helium main circuit, respectively. Based on indications from the literature, the calculation of temperature distribution was made on the assumption that 50% of the afterheat arises in the oxide, 30% in the metallic phase and 20% in the helium main circuit.

A first proposal for a possible concept of a core catcher is presented.

The calculation of the temperature distribution was based on a model in which a solidified fuel layer on the core catcher cooled at the bottom is followed by a stagnant liquid fuel layer, at the upper limit of which the maximum temperature of the melt is reached. This maximum temperature line represents the heat flux divide. Above this line heat in the liquid fuel melt will be transported upwards by natural convection. According to this model the steel layer is located above the fuel melt. Depending on the given heat production in the core melt, additional layers are found in the model of calculation. A numerical program was prepared which allows to calculate the temperature and heat flux distributions in the melt. The material data required for computation were taken from literature. In these initial computations values have been used which do not completely take into account the inter-actions of components present in the melt.

The results so obtained give already an indication of the design and tech-nological measures which are necessary to solve the problem of the molten core mass in a core catcher within the pressure vessel.

Temperatur- und Wärmeflußverteilung geschmolzener Core-Massen eines gasgekühlten schnellen Reaktors nach einem hypothetischen Niederschmelzunfall.

Zusammenfassung

Obwohl für einen richtig konzipierten gasgekühlten schnellen Brüter ein gleichzeitiger Abfall des Kühlmitteldruckes und Ausfall aller Kühlgebläse zu unglaubhaft erscheint, um als Auslegungsfall betrachtet zu werden, ist doch die Frage nach der Temperatur und Wärmestromverteilung in einer geschmolzenen Core-Masse, welche in einem Core-Catcher aufgefangen wird, von großem Interesse.

In diesem Bericht wurde angenommen, daß die geschmolzene Core-Masse sich nach 100 sec in dem Core-Catcher befindet und daß die Schmelze in eine oxidische und metallische Phase getrennt ist.

Die Spaltprodukte werden sich je nach ihrem Zustand entweder in dem oxidischen oder dem metallischen Teil der geschmolzenen Core-Masse bzw. in dem Gasraum befinden.

Basierend auf Angaben aus der Literatur, wurden die Rechnungen unter der Annahme durchgeführt, daß 50% der Nachwärme in der oxidischen, 30% in der metallischen Phase und 20% in dem Heliumprimärkreislauf freigesetzt werden.

Ein erster Vorschlag für ein mögliches Konzept eines Core-Catchers wird vorgestellt.

Die Berechnung der Temperaturverteilung basierten auf einem Modell, bei welchem auf eine erstarrte Brennstoffschicht auf dem Boden des von unten gekühlten Core-Catchers eine stagnierende flüssige Brennstoffschicht folgt, an deren Oberseite die maximale Temperatur der Schmelze erreicht wird. Diese Linie der maximalen Temperatur stellt die Wärmeflußscheide dar. Oberhalb dieser Linie wird die Wärme in der flüssigen Brennstoffschmelze durch Naturkonvektion aufwärts transportiert. In diesem Modell ist ferner angenommen, daß die Stahlschicht über der Brennstoffschmelze liegt. Je nach Größe der Nachwärmeleistung in der Core-Schmelze treten zusätzliche Schichten im Rechenmodell auf. Es wurde ein numerisches Programm erstellt, mit welchem die Temperatur- und Wärmeflußverteilung berechnet werden können. Die für die Berechnung erforderlichen Materialdaten wurden der Literatur entnommen. Für die ersten Rechnungen wurden Werte verwendet, bei welchen die Wechselwirkung mit den in der Schmelze vorhandenen Komponenten nicht voll berücksichtigt wurde.

Die so gewonnenen Ergebnisse geben jedoch schon Hinweise auf das Konzept und die technologischen Maßnahmen, die erforderlich werden, um das Problem der Bewältigung einer geschmolzenen Core-Masse in einem Core-Catcher innerhalb des Druckbehälters zu lösen.

1. Introduction

Although a core melt-down appear to be extremely unlikely in a properly designed
GCFR-system, it may be worth-while to investigate this problem since this question
has been raised for the Liquid Metal Fast Reactor as well.

The central problem in this context is how to contain, for a very long time, the
molten core mass on the floor of the reactor cavity in the prestressed concrete
pressure vessel. The knowledge of temperature and heat flux distribution in the
molten core mass contained in the crucible of the core catcher is necessary to
be able to design this catcher properly.

2. Core-catcher concept

Figure 1 shows the schematic outline of the core-catcher proposed for a GCFR.
The core catcher is planed on the floor of the reactor cavity of the concrete
pressure vessel. It is assumed that the molten core mass is fallen inside the
core-catcher and that the core debris can be cooled by all the sides. This is
essential if one wants to avoid that all the reactor cavity internals are melted
by the heat radiated by the molten core. As we will show later in the paper, the
heat radiated above the core debris is always considerably higher than the heat
flux going downward to the crucible, even with very effective floor cooling.

To increase as much as possible the heat flux going downward, we assumed that
the floor of the crucible was made of graphite, which among refractory materials
has a very good thermal conductivity, the lower surface of the graphite layer
being kept at $400^{\circ}K$ by cooling coils. To avoid formation of CO/CO_2 by the con-
tact of hot fuel (UO_2, PuO_2) with the graphite, the graphite floor is protected
by a tungsten liner.

3. Distribution of the Decay Heat Sources

As shown by the experiments of Fischer et.al. /1/, the fuel and steel of the
cladding are always separated, not only during the melt down, but also in the

core-catcher. Due attention must be paid to this fact in the assessment of the distribution of the fission products which constitute the decay heat sources.

Table I shows the fission products generated during operation of the reactor divided into three groups.

In the group A the fission products are listed which are gaseous or which have at the interesting temperatures such a high vapour pressure that they are volatile. A part of this fission products are released already during normal operation and collected in the venting system. A part will be released when the clad starts to fail and the rest will surely escape during the melt-down of the core. Thereby the condensable vapours will condense on the colder parts of the helium primary circuit, for istance on the liner of the concrete vessel or on the cold parts of the steel-graphite reflector.

The second group B includes such fission products, which have stable oxides in the interesting temperature range. Essentially these oxides are in homogeneous solution in the fuel melt.

In the last group C are listed the metallic fission products with low vapour pressure. Since these metallic fission products are very soluble in the molten steel, we will find these products mainly in the steel area. They are transported from the fuel to the steel with a time constant which depends on the transport mechanism from the melt to the fuel-steel interface. In the fuel layer this transport is controlled by natural convection and we can assume, according to Wantland and Fontana /2/, a fast separation of fission products.

On the basis of these considerations we assume that 50% of the decay heat due to the fission product group B is uniformely distributed in the fuel melt and 30%, due to the fission product group C, in the steel melt. We assume furthermore that this relation is constant over the time.

4. Steady State Temperature Distribution in the Core-Catcher

The investigation was made for a 1000 MWe Gas Cooled Breeder with steel clad
pins and oxide fuel /3/. It was assumed that the whole core, including the axial
and radial blankets, is molten down. With a surface of the crucible on the floor
of the reactor cavity of 40 m^2, we get the following layer thicknesses for the
melt:

- height of the fuel layer, including breeding material: h_{fuel} = 35.1 cm

- height of the steel layer : h_{ss} = 13.7 cm

4.1 Calculation Model

The melt in the crucible was divided into several layers, each of the layers
being characterized by its heat transport mechanism and by its state of aggre-
gation.

At the bottom of the crucible lies a (solidified) frozen fuel layer followed
by a stagnating liquid fuel layer, at the upper surface of which the highest
temperature will be reached. In these both layers the heat is transported only
by heat conduction and the temperature profile is parabolic. In the molten fuel
below the maximum temperature convection does not occur, because the buoyancy
forces are missing, due to the fact that the temperature at the top of the liquid
phase is the highest.

Above the molten stagnating fuel layer, another molten fuel layer follows, where
the heat is transported by natural convection. This convection is made up of
many little eddies (whirls) /4/, which form an hexagonal flow pattern (Benard-
celle). For such a flow, Nusselt numbers relationships for water with homo-
geneously distributed heat sources have been meassured and calculated /5/,
with which the temperature difference between the limits of the layer can be
calculated.

$$Nu = 0.177 \cdot Ra^{0,295} \tag{1}$$

where

$$Nu = \frac{\alpha \cdot s}{\lambda_{cond.}} = \frac{s^2 \cdot q_{fuel}}{2 \cdot \lambda_{cond.} \cdot \Delta T} \tag{2}$$

q_{fuel} = heat source density in the fuel $[W/cm^3]$

s = thickness of the convection layer $[cm]$

λ_{cond} = thermal conductivity $[W/cm \, ^\circ K]$

ΔT = temperature difference $[^\circ K]$

$Ra = \dfrac{g \cdot \beta \cdot T \cdot s^3}{\nu a}$ = Rayleigh-number

β = volume expansion coefficient $[^\circ K^{-1}]$

ν = kinematic viscosity $[cm^2/sec]$

a = thermal diffusivity $[cm^2/sec]$

The liquid convection layer is followed by a layer of solid fuel, where the heat is transported again only by conduction. In this layer the transport of heat is much less effective than in the convective layer, therefore this layer is much thinner than the convection layer. Because the density of the solid fuel is higher than that of its liquid phase, the forming of this layer is only possible as a result of a dynamic equilibrium between solid fuel particles falling down and fuel freezing at the interface. This layer dissappears at high heat fluxes. A layer of liquid steel through which the heat is transported by convection follows above this. To describe the heat transport herein the equation (1) is easily modified, to take into account that, in this layer, the heat flux resulting of the volume heat source and the heat flux coming out of the lower layers have to be added.

The core melt ends with a frozen steel layer in which heat is transported by conduction only.

The heat from the surface of this steel layer is carried off by radiation on the surrounding ambient, i.e. in our case on the cooled radiation shielding.

Depending on the value of the volume heat source, the layers of frozen fuel and frozen steel can disappear. With low heat fluxes all layers are solid. In the numerical calculations all these possibilities are treated by asking the value of the temperature at the interfaces.

4.2 Program

The problem is treated as one dimensional and stationary, i.e. no time dependenz effects like the establishing of the temperature profile are considered. This will be the object of future work. For the numerical calculations a FORTRAN-program was written. This gives the possibility to calculate the following:

1. The temperatures on the interfaces of the various layers.
2. The thickness of these layers
3. The heat fluxes at the bottom of the core-catcher and at the surface of the melt.

In the program the power densities in the fuel and steel melts can be optionally varied.

4.3 Materials Physical Properties

The physical properties of the materials required for the calculations are taken from the literature. The most important of these properties are summarized in Table II. For the first calculations reported here, only values of the pure materials are used. The influence of the fission products and all other impurities present into the melt by interaction with other materials are not considered here.

To investigate the influence of the uncertainty of the material properties on the results, the values of these have been varied during the calculations.

4.4. Results

Temperature profiles and heat fluxes are calculated for various power densities in the bed.

Fig. 2 shows a temperature distribution in the melt at a total delay heat of 15 MW ($\approx 0.6\%$ of reactor nominal thermal power) at which all possible layers are builded. In this case the highest temperature T_3 lies only 43 degree Kelvin over the melting point of the fuel.

On Fig.3, three temperature distributions are drawn for a total delay heat of 60 MW and 80 MW respectively. In these two last cases shown the upper layer of frozen fuel and steel do not appear. Fig.3 shows also the temperature distribution with 60 MW delay heat and a crucible having a thermal conductivity equal to only 1/5th of that a graphit. In Fig.4 the maximum temperatures in the fuel and in the steel T_3 and T_5 and the temperature of the surface of the crucible T_1 and of the surface of the melt T_7 have been plotted against the total delay heat P_{total}. The results show that above a total power of 10 MW the first liquid layers appear and that above 80 MW not only the fuel but also the steel begins to boil.

Boiling in the melting is being investigated now and will be the object of a future paper.

In Fig.5 the heat fluxes downward in the crucible and upward on the surface of the melt are plotted against the total delay heat. It is shown, that above the limit, where natural convection occurs, the heat radiated away by the melt upper surface is considerably greater than that which goes to the floor cooling coils. At 80 MW for istance the ratio J_o/J_7 is 0.184.

An increase of 100% in the values of the viscosity of the molten fuel and steel, which are affected with the greatest amount of uncertainty, produces an increase of the maximum temperature of the melt of only $96^{\circ}K$.

5. Conclusions

The calculation show, that at higher total delay heat maximum temperatures are reached, which lie over the boiling points of both steel and fuel. Further it is shown, that the greatest part of the delay heat, also for the case of boiling is radiated away at the upper surface of the melt. In the design of the core-catcher one has therefore to pay the greatest attention to shielding of this heat flux to avoid the melting of the reactor cavity internals.

References

/1/   J.FISCHER, J.D.SCHILB and M.G.CHASANOV, Investigation of the
       Distribution of Fission Products among Molten Fuel and Reactor
       Phases, ANL-7864 (1971)

/2/   J.L.WANTLAND and M.H.FONTANA, Enhancement of Heat and Mass Transfer
       by Internal Convection in Molten Cores, ORNL 4374

/3/   Gasbrüter-Memorandum, KFK 1375

/4/   P.L.SILVESTON, Wärmedurchgang in waagrechten Flüssigkeitsschichten,
       Forsch.Ing.Wes.Bd. 24 (1958)

/5/   H.E.FIEDLER and R.WILLE, Turbulente Freie Konvektion in einer
       Horizontalen Flüssigkeitsschicht mit Volumen-Wärmequelle,
       Heat Transfer 1970, Vol.IV.

TABLE I Fission-Product Decay Heat [*]

Fission-product Element	Percent of Total Heat at 85 sec after Shutdown
Group A	
I	11.1
Cs	6.9
Kr+Xe	6.5
Sb	3.9
Te	3.3
Group B	
Y	7.8
La	7.6
Sr	4.5
Ba	3.9
Zr	2.8
Pr	3.6
Ce	2.2
Nb	8.0
Group C	
Nb	-
Mo	6.0
Tc	8.0
Ru	2.7
Rh	2.0
Other elements each	<1.0

[*] J.FISCHER, J.D.SCHILB and M.G.CHASANOV, Investigation of the Distribution of Fission Products among Molten Fuel and Reactor Phases, ANL-7864

TABLE II Physical Properties of Fuel and Stainless Steel for the Calculation of the Temperature Profile in the Core-Melt.

Property	Value	Reference	Year	Remarks
Thermal conductivity of $(U_{0.8}Pu_{0.2})O_2$ near the melting point (Slightly above or below) $\lambda \left[\dfrac{W}{cm\,^{\circ}K} \right]$	2.09×10^{-2}	ANL-7859, S.27 ANL-7947, S.1o2	1969	
	3.0×10^{-2}	GEAP-13733	1971	Extrapolation of H.Friedrich, Siemens (10.10.72)
	4.75×10^{-2}	AI-TI-015-23-052	1970	molten fuel
	$\underline{3.5}^{\ast} \times 10^{-2}$	Atomwirtschaft 17 (1972) S.37	1972	molten fuel at 2800°C
	$\underline{3.415} \times 10^{-2}$			solid fuel
Specific Heat of $(U_{0.8}Pu_{0.2})O_2$ near the melting point $c_p \left[\dfrac{W\ sec}{gr\,^{\circ}K} \right]$	0.460	ANL-7947, S.1o2 GEAP-10059	1969	for UO_2
	0.521	ANL-7800 ANL-RDP-2	1971 1972	for UO_2 for UO_2
	$\underline{0.513}$	ANL-7610	1970	for $T > 3115\,^{\circ}K$

* The underlined values are those adopted in the calculations.

Property	Value	Reference	Year	Remarks
Density of liquid $(U_{0.8}Pu_{0.2})O_2$ $[gr/cm^3]$	8.7	ANL-RDP-2	1972	for UO_2 at 2800°C
	8.8			from various sources for $(U_{0.8}Pu_{0.2})O_2$ at 2800°C according to Friedrich, Siemens (10.10.72)
	8.74	ANL-7610, S.337	1970	
Heat of fusion $q_m \left[\dfrac{W\ sec}{gr}\right]$	282	ANL-7800	1971	for UO_2
Boiling point of $(U_{0.8}Pu_{0.2})O_2$ $[°C]$	3179	ANL-7859, S.27	1971	
	3200	ANL-RDP-2, S.8, 36	1972	
	3300	UKAEA (Farmer)	1972	private communication from Friedrich
	3450	ANL-7750, S.59	1970	for UO_2 extrapolated
	3816	AJ-TI-095-23-052	1970	Author unknown
Dynamic viscosity of liquid $(U_{0.8}Pu_{0.2})O_2$ $\eta \left[\dfrac{gr}{cm\ sec}\right]$	1.00	AJ-TJ-095-23-052	1970	Author unknown
	0.46	ANL-RDP-2	1972	for UO_2 at 2800°C

Property	Value	Reference	Year	Remarks
Kinematic viscosity of $(U_{0.8}Pu_{0.2})O_2$ $\nu = \dfrac{\eta}{\rho} \left[\dfrac{cm^2}{sec}\right]$	4.1×10^{-2}	BNWL-1279		$2795^{\circ}C$
Volume expansion coefficient of liquid $(U_{0.8}Pu_{0.2})O_2$ $\beta \left[\dfrac{1}{K}\right]$	1×10^{-4}	HW-76559, S.113	1963	UO_2
	1.05×10^{-4}	AI-TI-095-23-052	1970	assumed for $(U_{0.8}Pu_{0.2})O_2$
	1.05×10^{-4}	ANL-7610, S.337	1970	
Thermal conductivity of stainless steel near the melting point (slightly above or below) $\lambda \left[\dfrac{W}{cm\ ^{\circ}K}\right]$	0.3	Thyssen	1969	extrapolated from $900^{\circ}C$ for 1.4948
	0.26	DEW-Techn.Ber. 9.Bd.Heft 2	1969	ectrapolated from $1000^{\circ}C$ for 1.4981
	0.42	Arch. Eisenhütten-wesen, 41(1970) S. 965	1970	for fraze iron 1536 - $2027^{\circ}C$
	0.242			$800^{\circ}C$

Property	Value	Reference	Year	Remarks
Specific heat of stainless steel near the melting point (slightly above or below) $c_p \left[\dfrac{W\ sec}{gr\ {}^{\circ}K}\right]$	0.65 - 0.8	Information from various firms for 1.4948, AISI 304, AISI 347		steel solid at 1400°C
	0.72 and higher			steel liquid at 1500°C
	0.58	DEW-Techn.Ber. 9. Bd., Heft 2	1969	extrapolated from 1000°C for 1.4981
	0.749	Bull. 605, Bureau of Mines		
Density of liquid steel $\rho\ \left[gr/cm^3\right]$	7.2	Transact.of Met. Soc.AIME 224(1962) S.818 Nucl.Sci.Eng. 18 (1964) 280	1962 1964	
Heat of fusion of stainless steel 1.4948 1.4988 $q_m \left[\dfrac{W\ sec}{gr}\right]$	210 ÷ 290	various standard publications		

Property	Value	Reference	Year	Remarks
Boiling point of stainless steel $[^{o}C]$	Fe : $3000^{o}C$ Ni : $2900^{o}C$ Cr : $2480^{o}C$	Handb.of Chem.and Phys. The Chem.Rubber Publishing Co.(1963)	1963	
Dynamic viscosity of liquid stainless steel $\eta \left[\dfrac{gr}{cm\ sec} \right]$	4.76×10^{-2}	Arch.Eisenhüttenwesen 41 (1970)S.965	1970	average temp.of $1627^{o}C$
Volume expansion coefficient of liquid steel $\beta \left[\dfrac{1}{^{o}K} \right]$	1.157×10^{-4}	Transact. of Met.Soc.AIME 224 (1962) 818	1962	
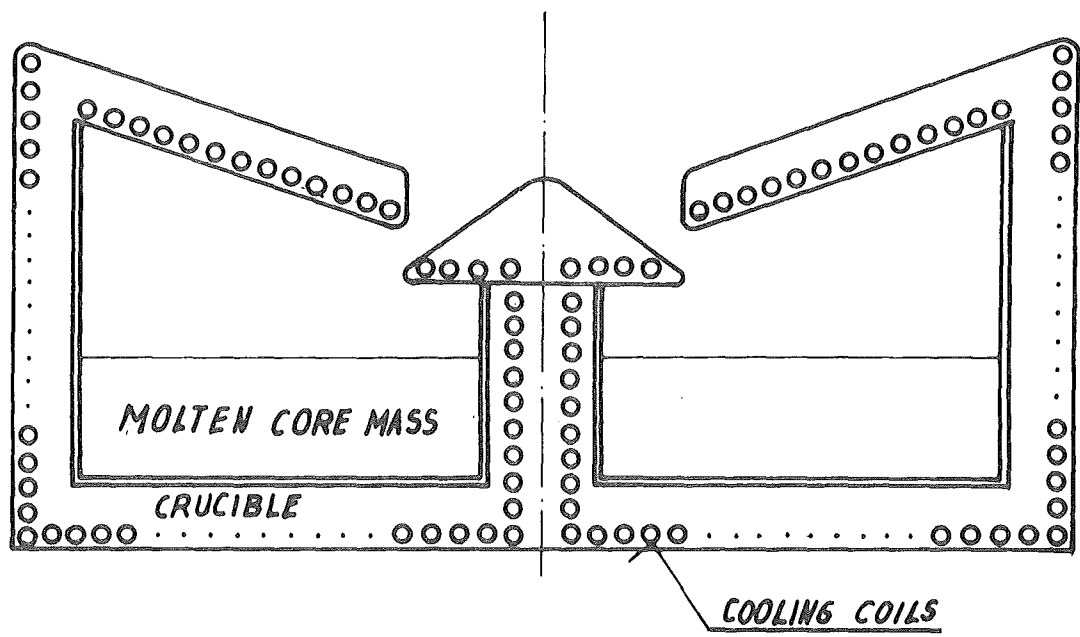
Fig. 1.   Core-catcher concept for a GCFR.
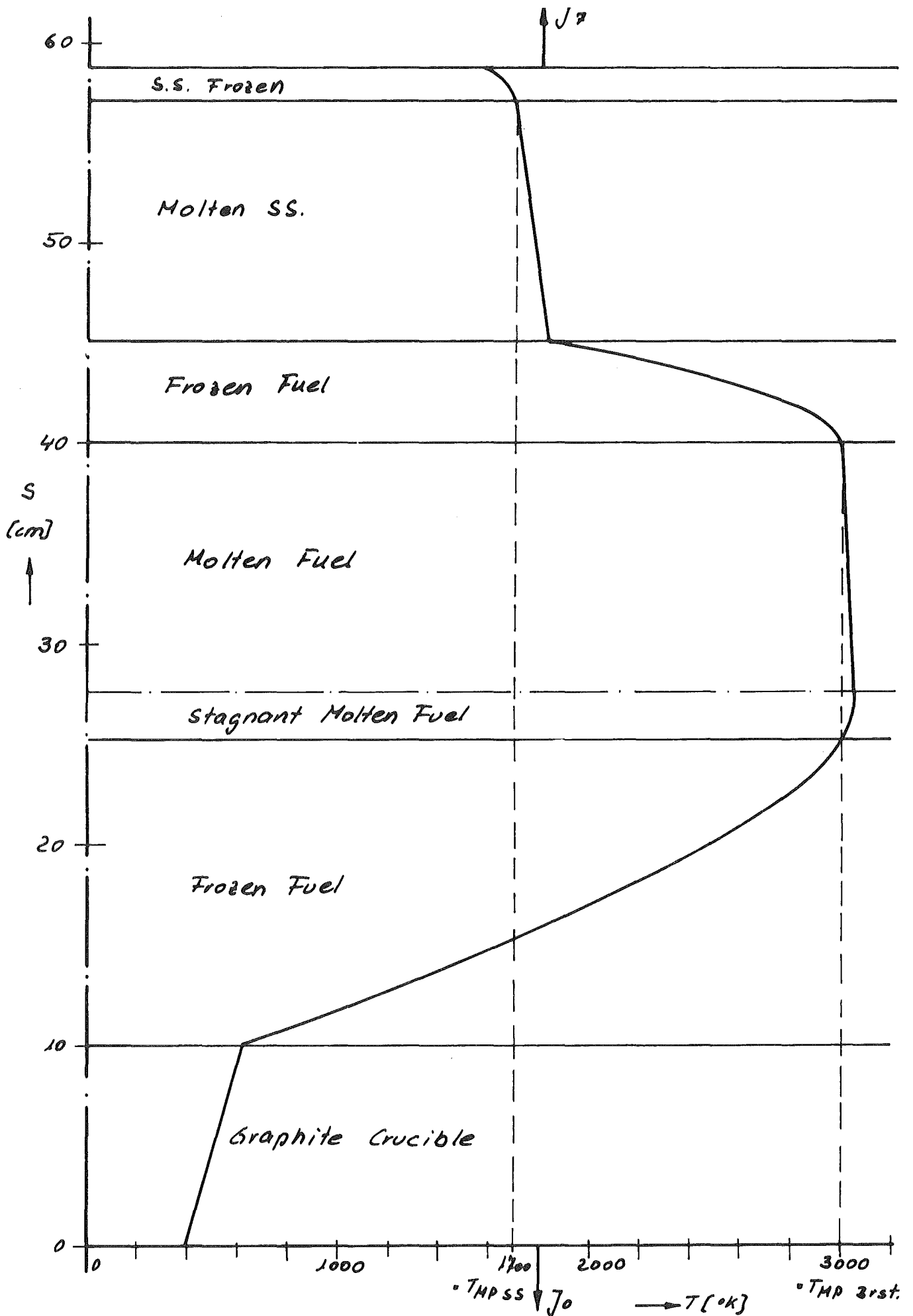Schematic outline

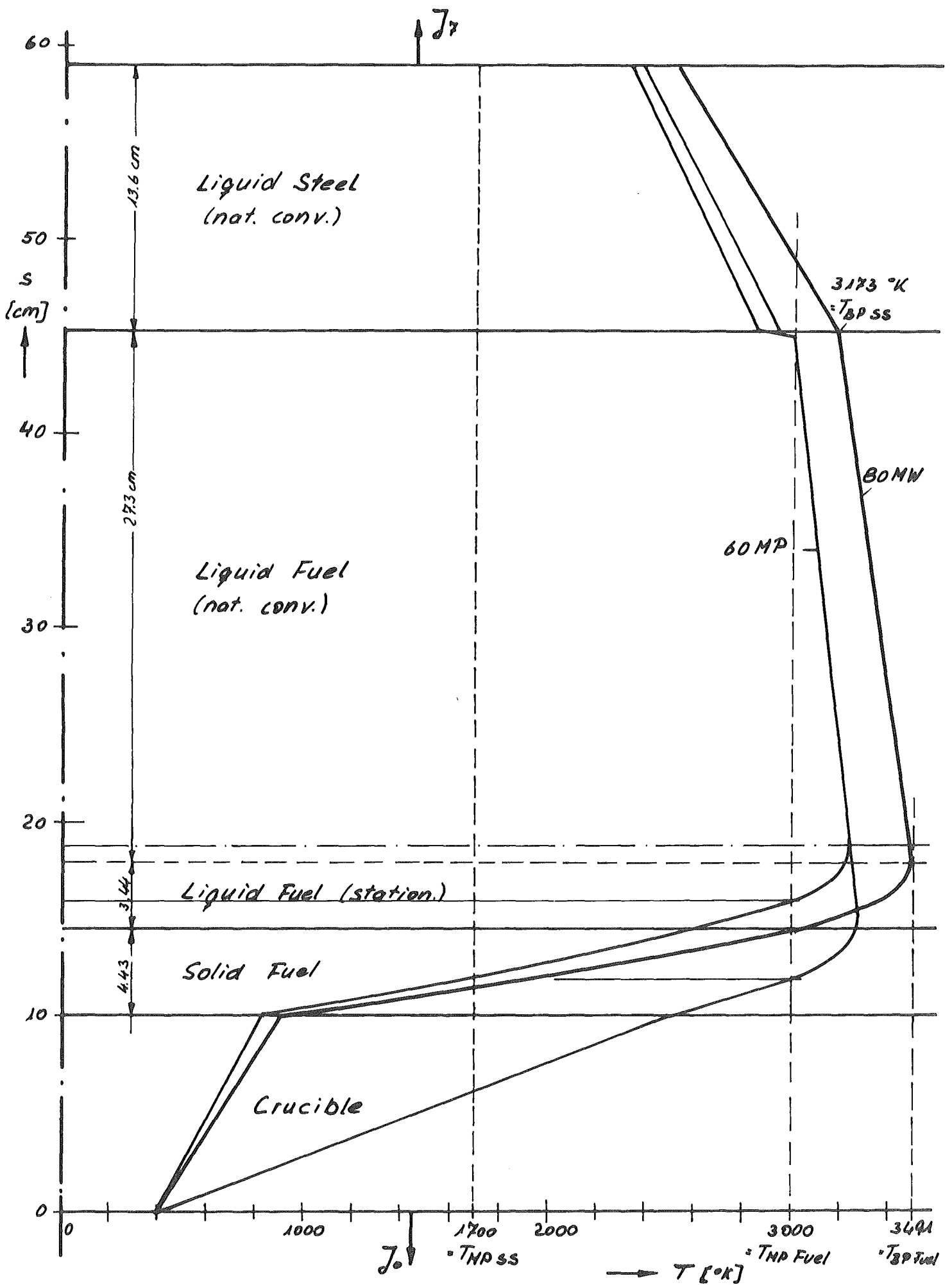Fig. 2   Temperature profile in the core melt
Total delay heat : 15 MW

Fig. 3 Temperature profile in the core melt
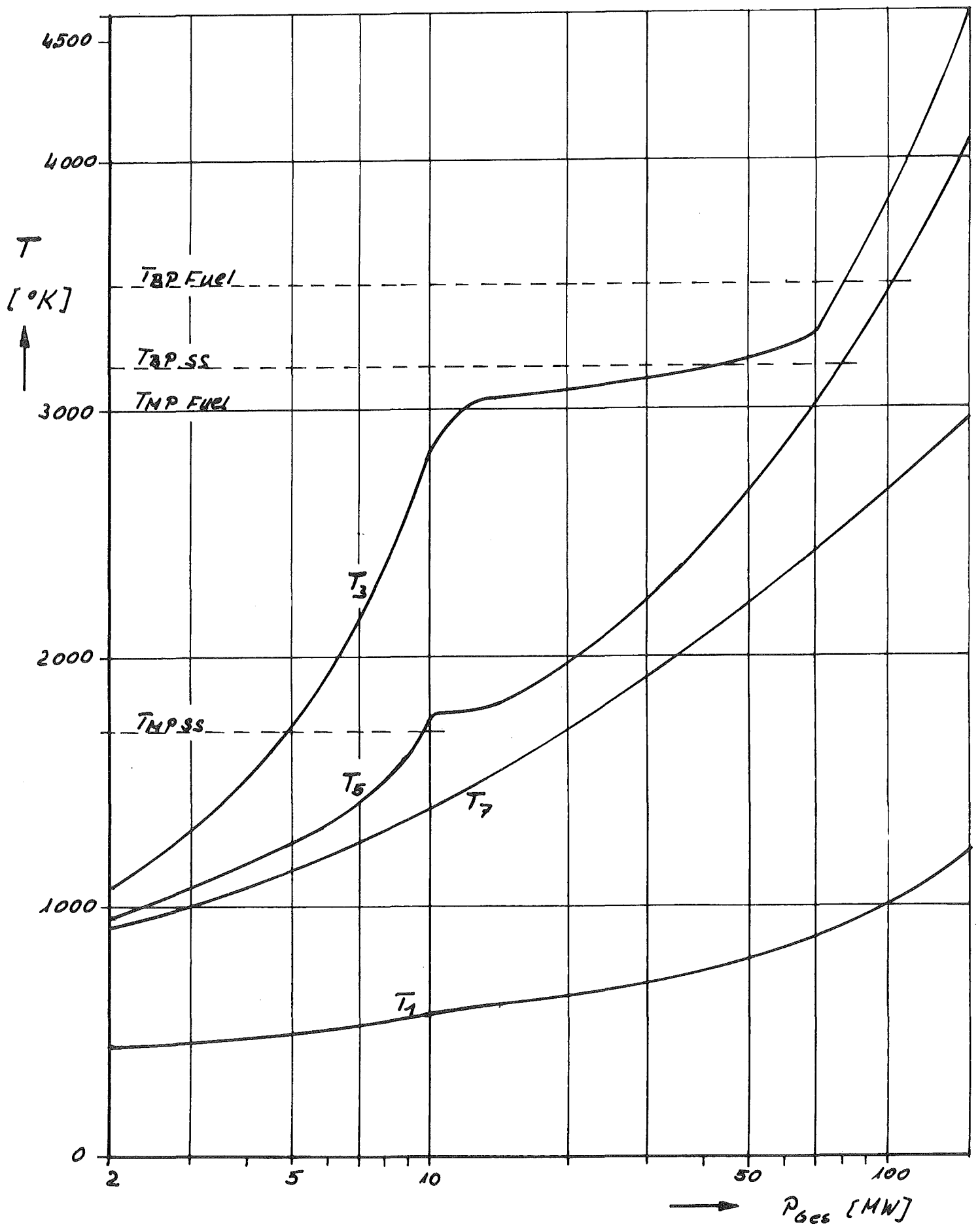After heat : 60 and 80 MW

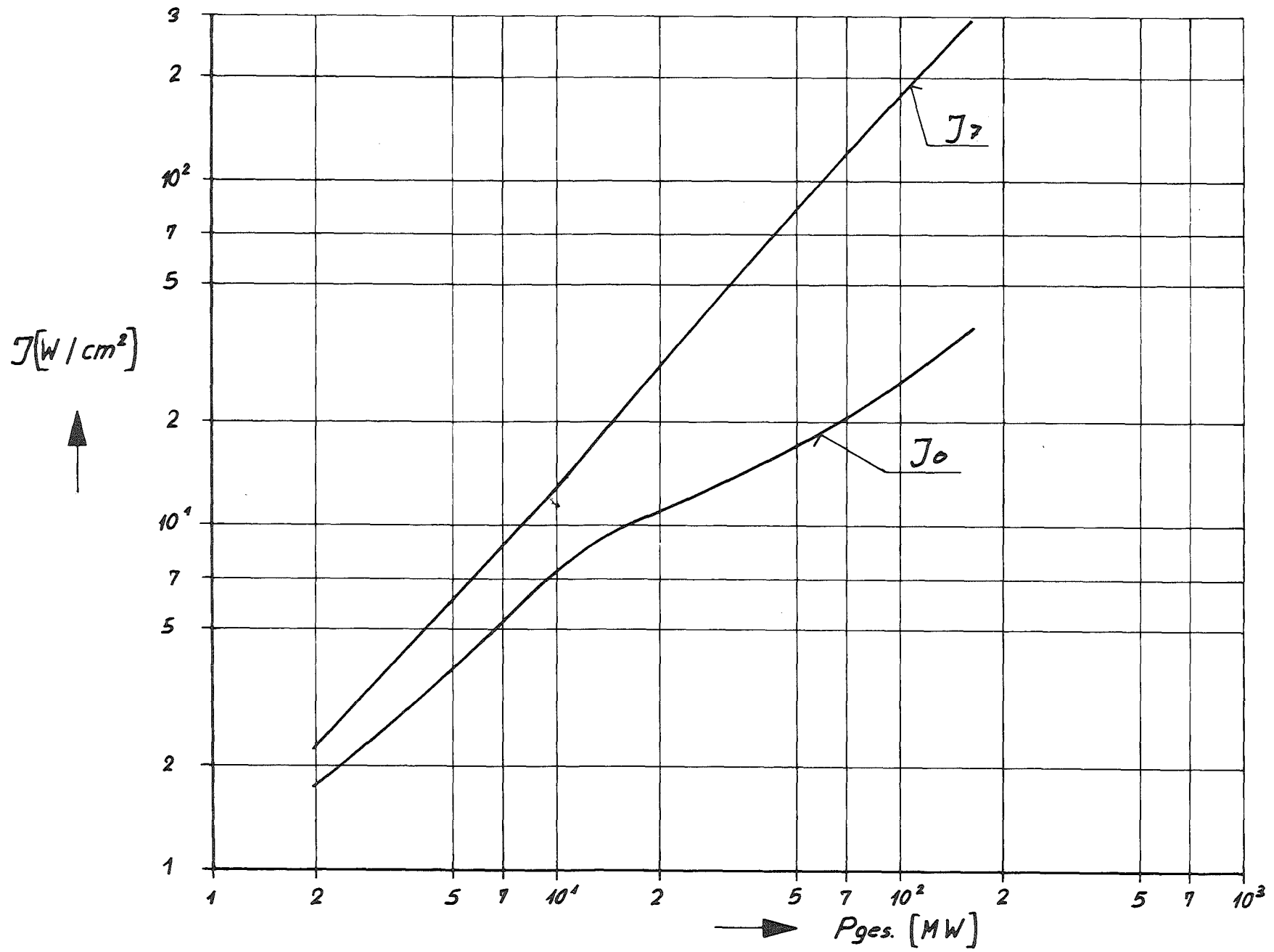Fig. 4 Relation between total delay heat and temperature in the core-catcher.

Fig. 5. Relation between heat-fluxes and total delay heat in the core-catcher